Science Press

ARTICLE

Molecular Dynamics Simulation of Tension of Al₂Cu with Voids

Liu Xiaobo,   Xiong Zhen,   Fang Zhou,   Li Yan

Nanchang Hangkong University, Nanchang 330063, China

Abstract: A molecules dynamic simulation model was established to simulate the tension of Al₂Cu with voids at normal temperature and constant engineering strain rate. The influence of void size, quantity and its distribution on the mechanical properties of Al₂Cu was studied by embedded atomic method. The results show that the void causes the appearance of free surface in the model and stress concentration at the inner edge of void, which greatly reduce the tensile strength and deformation ability of the material. In addition, the plastic and tensile strength of Al₂Cu decrease obviously with the increase of void size. The stress-strain curves corresponding to different numbers of voids basically overlap in the elastic deformation stage, and for more voids, the plasticity and tensile strength decrease. According to the change of void distribution, it can be found that the smaller the angle between the connection direction of the voids and the tensile direction, the stronger the plasticity and tensile strength of Al₂Cu.

Key words: molecular dynamics simulation; tension; void size; void number; void distribution

The 7XXX aluminum alloy belongs to Al-Zn-Mg-Cu superhard aluminum, which has the advantages of small density, high yield limit, and good processing performance. It is widely used in aerospace, defense, transportation and other industries. However, there are a great deal of coherent and incoherent second phase particles distributed in the 7XXX aluminum alloy matrix[1,2], which has a great influence on the recrystallization, mechanical property, fracture toughness and corrosion resistance of materials[3,4]. Therefore, the second phase particle Al₂Cu has been studied. Through the study of Al₂Cu in Al-Cu alloy, Gao et al[5] found that the growth behavior of Al₂Cu in different growth stages is different, and the ability of the eutectic synusia' nucleus formation of the primary crystal phase Al₂Cu is stronger than that of the primary crystal phase α-Al. According to the study of microstructure evolution and orientation analysis of hypereutectic Al-Al₂Cu alloy under directional solidification, Gao et al[6] found that there is similarity and difference in dendritic growth mechanism of Al₂Cu phase under the condition of directional solidification and abrupt growth rate, and the directional solidification process parameter is the dominant factor affecting the fi-

nal morphology and growth direction of dendrites. Tian et al[7] investigated the structural, mechanical and thermodynamic properties of Al₂Cu phase, and found that pressure can improve the elastic anisotropy, and thermal expansion coefficient is more sensitive to changes in pressure than in temperature within the temperature range of 300~800 K. Lombardi et al[8] researched the influence of Al₂Cu morphology on the incipient melting characteristics in B206 Al alloy. Sadeghi et al[9] used finite element and finite difference modeling methods and a lognormal distribution function to evaluate the effect of the particle size distribution on the dissolution behavior of the Al₂Cu particles. Research has shown that the dissolution kinetic is not affected by the particle-matrix interface, and the effect of the particle size distribution instead of an average particle size is taken into account.

As an important strengthening phase in 7XXX aluminum alloy, Al₂Cu has very poor plasticity, and the micro cracks may appear under low stress, accompanied by the generation of voids. The nucleation, growth and aggregation of voids are generally considered to be the main cause of ductility damage of plastic materials, and also a decisive factor affecting the

strength of materials[10,11]. Therefore, it is necessary to understand the influence regularity of these micro void defects on the properties of the alloy.

In recent years, the continuous development of computers provides a powerful tool for studying the microscopic characteristics of materials. Molecular dynamics has been proven to be an effective method for the realization of this goal. It can study the dynamic evolution process of a system from micro scale, and accurately grasp the rules of micro-level, such as the effect of stretching on the evolution of voids. At present, considerable researches have been performed on the molecular dynamics simulation of the stress and strain of materials without voids under tensile conditions[12-18]. As for the research of crack propagation of materials with voids, Chen et al[19] simulated the dynamic behavior of metal materials with voids under shock loadings, and found that the main reason for the formation of local hot spots during the process of void collapse is the appearance of micro-jet atomic compression. Besides, the dislocations and hot spots induced by void collapse have been proved to be associated with the formation of the local adiabatic shear band. Eduardo et al[20] have studied the launch and outward expansion of special dislocation loops by molecular dynamics simulation, and revealed that the critical stress of the void nucleation and growth in nanocrystals is much smaller than that of the effective nucleation position in the grain boundary of single crystal. Tapan et al[21] performed molecular dynamics simulations for the single crystal UO_2 with voids of 2.2 nm in diameter, and found that there will be a crossover between the surface-diffusion-controlled mechanism and the lattice-diffusion-controlled mechanism when void size is in micron level. Zeng et al[22] studied the plastic deformation of magnesium alloys near a atomic scale void by molecular dynamics simulation. The simulation results revealed that the passivation around the void, emission of dislocation, coalescence of void, and the micro void are the major factors contributing to the void growth. Zhang et al[23] simulated bi-crystal copper with voids under uniaxial tension by molecular dynamics simulation, and investigated the effects of two kinds of voids which are inside the grains and on the boundary on the mechanical behaviors of bi-crystals. Simar et al[24] studied the interaction between the edge dislocations in the decomposition of single crystal nickel when slip occurs and voids, and indicated the effect of the void size, detachment mechanism and dynamic response mechanism of the dislocation on the obstacle of material strength. Consequently, it was observed that the void strength increases with

increasing the void size. Liu et al[25] researched the void growth and interaction in a single crystal silicon cubic box under hydrostatic tension by performing three-dimensional strain-controlled molecular dynamics simulation. It was found that the silicon cube tends to fracture via void coalescence when the distance between voids is less than the critical initial inter-void ligament distance. These results confirm that molecular dynamics is an effective method to study the evolution of micro void defects in metallic materials.

However, the aforementioned researchers merely explored crack propagation behavior by studying crack or void. In other words, it only focused on the regularity of crack propagation without considering the influence of stretching on stress and strain of the material with voids. Hence, this paper used LAMMPS molecular dynamics software and EMA (embedded atom model) potential function to simulate the tensile deformation of Al_2Cu with voids, and then analyzed its mechanical property of Al_2Cu. The trajectory map of the atomic special time system was obtained by visual software OVITO so that the deformation of Al_2Cu under tensile load can be observed clearly.

1   Establishment of Model

The related parameters of Al_2Cu cell structure are shown in Table 1.

According to the relevant parameter of Al_2Cu, crystal cell structure is established, as shown in Fig.1. *X*, *Y* and *Z* correspond to crystal orientation [100], [010], and [001], respectively.

After the unit cell is established, the Al_2Cu cell is loaded through the read_data function of LAMMPS. The periodic boundary condition is given and repeated 10 times in the direction of *X*, *Y*, and *Z*. The initial simulation model of $10a_0 \times 10a_0 \times 10b_0$ is established, as shown in Fig.2a. There are 12 000 atoms in this model system, the actual size of the model is 6.07 nm×6.07 nm×4.88 nm, and its volume and symmetry space group name are 179.515 nm³ and H-M 'I4/MCM', respectively. a_0 and b_0 are the lattice constants of Al_2Cu at a certain temperature[26]. In order to balance the system, the initial model would be relaxed in the hot bath of 300 K with 50 000 steps, and the time step was chosen to be 0.001 ps. Then, a circular region with a radius of $1a_0$ was established at the center of the model ($5a_0$, $5a_0$, $5b_0$), and delete_ atom command was used to delete 61 atoms, which prefabricated a void with a radius of approximately 1.21 nm. The model has a total of 11 939 atoms, and the whole model and the sectional drawing of the center are shown in Fig.2.

Table 1   Lattice parameters of Al_2Cu cell

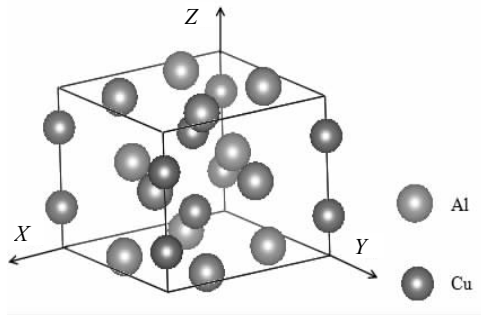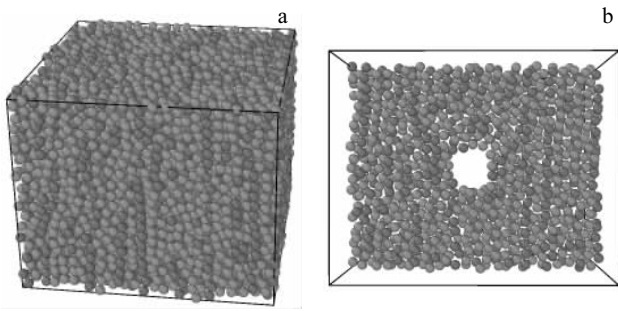| Lattice parameters				Cell angle/(°)			Symmetry space group H-M'I4/MCM'			
a/nm	*b*/nm	*c*/nm	Volume/nm³	α	β	γ	Atom	*X*	*Y*	*Z*
6.067	6.067	4.877	179.515	90	90	90	Cu	0.00000	0.00000	0.25000
							Al	0.15810	0.65810	0.00000

Fig.1   Diagrammatic sketch of cell structure of Al₂Cu

Fig.2   Simulation model diagram of initial model containing prefabricated void (a) and sectional drawing of the center void (b)

2   Potential Function of Molecular Dynamics Simulation

Potential functions describe interactions between atoms, which control their interactions and fundamentally determine all the properties of the material. In molecular dynamics simulation, the correct selection of potential function plays a decisive role in the simulation results. The EAM potential function[27,28] is used to simulate the interaction between Al₂Cu atoms. The total potential energy of the system is:

$$U = \sum_i F_i(\rho_i) + \frac{1}{2}\sum_{j \neq i} \phi_{ij}(r_{ij}) \qquad (1)$$

$$\rho_i = \sum_{\substack{i,j \\ i \neq j}} f_j(r_{ij}) \qquad (2)$$

where ρ_i means the charge density generated by all the atoms except the atom i at the atomic i; $f(r)$ is the electron density distribution function of atoms; r_{ij} is the distance between the ith atom and the jth atom.

3   Results and Discussion

3.1   Tensile results and analysis of Al₂Cu with prefabricated voids at normal temperature

The obtained model is uniformly stretched along the X axis

at constant temperature of 300 K. In order to ensure the accuracy of calculation, the whole system deforms once every run time step. The engineering strain is 0.001 ps⁻¹, and the entire program runs 200 000 steps. During this period, the coordinates, strain rate, temperature, kinetic energy, potential energy and stress of the atom are recorded every 200 steps.

The stress and strain data obtained by operation are plotted as the stress-strain curve, shown in Fig.3. After the atomic trajectory information is processed by the visual software Ovito, the crack propagation trajectory of atomic system at special time is shown in Fig.4, and then the corresponding two diagrams are analyzed.

As shown in partial magnification of Fig.3, the initial stress of the model containing a prefabricated void is not 0 because the inner edge of the prefabricated void is the same as the free boundary condition. The atoms on the inner edge of the void lose their adjacent atoms in space and produce a broken bond, which results in difference between the coordination numbers of atoms in the inner edge of the void and that of the other atoms inside, and therefore the former has a higher surface residual energy. Since the force symmetry is broken away from the ideal equilibrium position, surface tension is caused, and the stress in the tensile direction of the atom is not 0 under the initial relaxed unloaded condition.

The stress-strain diagram of Al₂Cu with voids is similar to that without voids. In the initial stage of tension, as shown at 'a' in Fig.3, there is an elastic deformation stage, and the stress-strain relation approximates a straight line. Stress increases linearly with increasing the strain. The linear relationship reflected by Hooke's law is still formed in this range, and the elastic modulus of the material can be calculated accordingly. As shown in Fig.4a, as the stretching continues to $\varepsilon=0.0450$, the void is slightly larger than that without stretching and the deformation of the system is still dominated by elastic deformation with a small amount of plastic deformation. With the further increase of tensile strength to 3.52 GPa, when $\varepsilon=0.0498$, the system stress begins to decline rapidly. Meanwhile, the rapid growth of the void can be found at this point from the atomic trajectory map, and the plastic deformation increases. It should be noted that the atomic lattice in the inner edge of the void is rearranged constantly to release the strain energy and a disordered area is formed due to the launch of dislocation. When the strain loads into phase between $\varepsilon=0.0740$ and $\varepsilon=0.0780$, the stress after a short period of plateau is roughly stable at 2.5 GPa, as shown at 'b' in Fig.3. Fig.4b presents the atomic trajectory map for the loaded strain of $\varepsilon=0.0760$. It can be found that the growth rate of the void along the [001] direction is significantly greater than that along the [00$\bar{1}$] direction, and the propagation speeds in different directions are different, which results in the roughness of the edge of the void. As shown at 'c' in Fig.3, the stress-strain curve moves through two small fluctuations at $\varepsilon=0.110$ and $\varepsilon=0.127$ as the loading continues. With the continuous
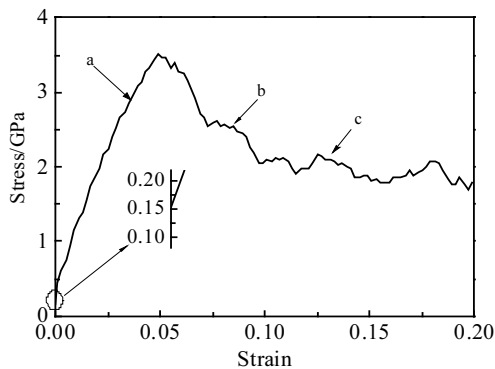
Fig.3   Tensile stress-strain curve of the model containing a prefabri-cated void with 1.21 nm in radius

decline of stress, its level fluctuates around 2 GPa when the strain develops to $\varepsilon=0.1346$, as shown in Fig.4c, and the value is leveled off. The strain at this time is nearly two times larger than that in Fig.4b, but the void growth is not obvious, and the disorder of atoms in the inner edge of the void decreases accordingly.

Fig.5 presents the stress-strain curves of Al_2Cu with and without prefabricated voids. After comparison, it can be seen clearly that the tensile strength of the simulation system decreases by nearly half after adding a prefabricated void with a diameter of 1.21 nm, that is, 6.4 GPa to 3.45 GPa. The strain of the tensile strength also decreases from $\varepsilon=0.086$ to $\varepsilon=0.0498$. This is because of the existence of stress concentration area in the inner edge of the void, which greatly reduces the stress required for slip. Moreover, the prefabricated void gives a larger internal space for the simulated material, making the multiplication process of dislocation easier. It can also be seen from Fig.5 that the elastic modulus of the model without a prefabricated void is higher than that with prefabricated void, and the stress of the model without prefabricated void decreases rapidly to 2.25 GPa after the stress reaching the tensile strength. However, the stress of the model with a prefabricated void decreases gently with the increase of strain after reaching the tensile strength, and a platform emerges when the stress decreases to 2.5 GPa at strain $\varepsilon=0.070$. After a very short loading, the stress of the model with a prefabricated void falls to 2.0 GPa and almost remains at this value until the end of simulation. In general, the presence of the void causes the free surface to appear inside the model and the stress concentration is generated in the inner edge of the void, thus greatly reducing the tensile strength and deformation ability of the material.

3.2   Influence of the prefabricated void size on the tensile results of Al_2Cu

In order to study the influence of void size on the tensile mechanical properties of Al_2Cu, 5 prefabricated voids with different sizes were set up to simulate and to facilitate the comparison of the void with a radius of $1a_0$ set by the initial

model of $10a_0 \times 10a_0 \times 10b_0$. Then a circular region where each void is located was set up at the center of the model ($5a_0$, $5a_0$, $5b_0$), and delete_atom command was used to delete the corresponding number of atoms, prefabricating 5 voids with different radii of $1a_0$, $1.5a_0$, $2a_0$, $2.5a_0$ and $3a_0$. The specific number of atoms to be deleted, the number of atoms left, the atomic deletion rate, the radius of the hole and the actual size are shown in Table 2, while other simulation parameter settings remain unchanged.

Under the condition of 300 K constant temperature, the whole system is stretched along the *X*-axis, with the engineering
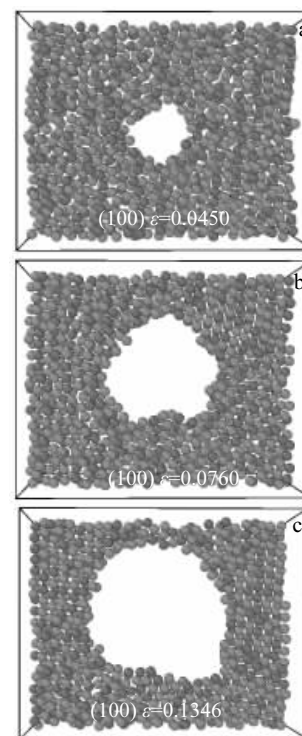

Fig.4   Atomic trajectories map at different strains: (a) $\varepsilon=0.0450$, (b) $\varepsilon=0.0760$, and (c) $\varepsilon=0.1346$
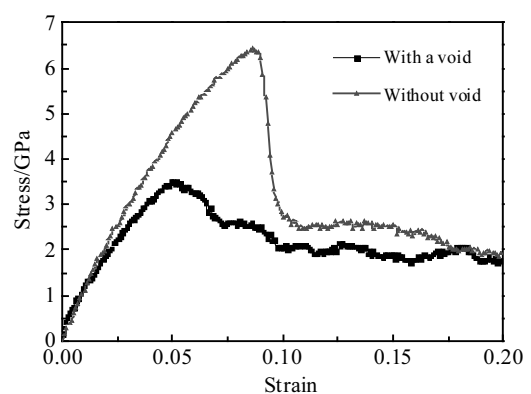

Fig.5   Stress-strain curves of Al_2Cu with and without prefabricated voids

Table 2　Relevant parameters of molds with voids of different sizes

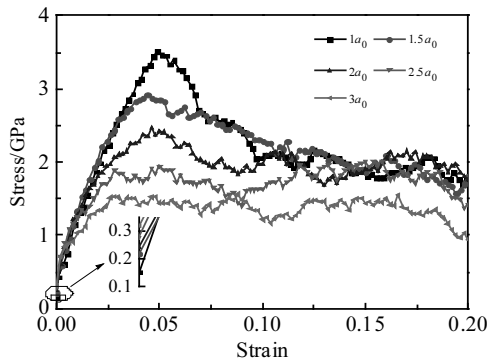| Radius of the void, R	$1a_0$	$1.5a_0$	$2a_0$	$2.5a_0$	$3a_0$
Actual diameter/nm	1.21	1.82	2.43	3.03	3.64
Number of atoms to be deleted	66	202	487	952	1642
Number of atoms left	11 934	11 798	11 513	11 048	10 358
Atomic deletion rate/%	0.55	1.68	4.06	7.93	12.68

Fig.6　Stress-strain diagram corresponding to the voids with different radii

strain of 0.001 ps⁻¹ and the program running 200 000 steps. The coordinates, strain rate, temperature, kinetic energy, potential energy and stress of the atom are recorded every 200 steps during this period. Fig.6 shows the stress-strain curves corresponding to the voids of different radii.

It can be seen from Fig.6 that the initial stresses of the void with different sizes are different. The minimum initial stress of the void is 0.15 GPa, corresponding to the void with a radius of $R=1a_0$. The initial stress increases with the increase of the radius of the void, and the initial stress reaches 0.32 GPa when $R=3a_0$. This is because the existence of prefabricated void introduces the free surface to the whole model system. The atoms on the free surface, i.e., the atoms on the inner edge of the void, lose their adjacent atoms in space and produce the broken bond. As a result, the coordination number of atoms in the inner edge of the void is different from that of other atoms inside, and therefore the former has a higher surface residual energy. Since the force symmetry is broken off the ideal balance position, the surface tension is generated. The larger the prefabricated void, the more free surface and the larger the pre-stressing force. Hence, the initial stress increases with the increase of the radius of the void.

After comparing the stress-strain curves corresponding to prefabricated voids with different sizes, it can be found that the stress and strain are in a linear relation when the radius of the prefabricated void is $1a_0$, and the system has an elastic deformation. When the radius of the prefabricated void is $3a_0$,

this elastic deformation stage is hardly observed from the stress-strain curve. Hence, it can be concluded that the elastic deformation stage is less obvious with the increase in the size of the prefabricated void. This may be due to the fact that the larger prefabricated voids introduce larger internal space to the system, which makes slippage easier, and thus plastic deformation takes place under low stress.

As the stretching proceeds, the stress in the system of the prefabricated void with a radius of $R=2.5a_0$ and $R=3a_0$ does not attain an apparent peak, but it fluctuates at 1.4 and 1.75 GPa after loading to the strain $\varepsilon=0.03$, until the simulation is completed. This may be due to the plastic flow in the system, which is a very complicated process involving the interaction between a large number of dislocations.

As can be seen from the diagram, the corresponding tensile strength also decreases to different degrees with the increase of prefabricated void size. The tensile strength of prefabricated void with a radius of $R=1a_0$ reaches 3.52 GPa at $\varepsilon=0.0498$, while that of the void with a radius of $R=1.5a_0$ reaches 2.82 GPa at $\varepsilon=0.0470$, and the tensile strength of prefabricated void with a radius of $R=1.5a_0$ reaches 2.50 GPa at $\varepsilon=0.0468$. After reaching the tensile strength, the decrease trend of the stress-strain curves is gradually flattened with the increase of void radius. Meanwhile, more obvious fluctuations exist in the corresponding stress-strain curve. Due to the simultaneous increase of atomic deletion rate, it is impossible to determine whether the fluctuation is caused by the size of the void or by atomic deletion rate.

3.3　Effect of the number of prefabricated voids on Al₂Cu tensile results
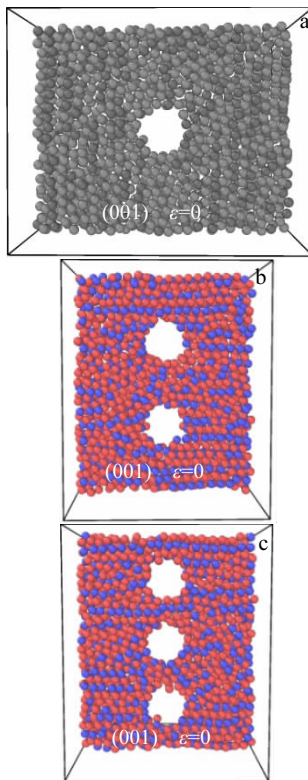
In order to simulate the influence of the number of voids on the tensile mechanical properties of Al₂Cu, 3 models of $10a_0\times10a_0\times10b_0$ are built, and 1, 2, 3 voids with radius of $R=1a_0$ are set in them. The void positions and related parameters of each model are listed in Table 3, and the initial models are shown in Fig.7.

The obtained model is uniformly stretched along the X-axis at 300 K constant temperature. The whole system deforms once every run time step. The engineering strain is 0.001 ps⁻¹, and the whole program runs 20 000 steps. During this period, the coordinates of the atoms, strain rate, temperature, kinetic energy, potential energy and stress are recorded every 200 steps.

The stress and strain data obtained by operation is plotted as the stress-strain curves shown in Fig.8. It can be found that the initial stress of the model containing prefabricated voids is not zero, because the inner edge of the prefabricated void is equivalent to the free boundary condition, which results in surface tension. The stress-strain curves corresponding to different numbers of voids are basically coincident in the elastic deformation stage. As the tension continues, the model with 3 prefabricated voids firstly reaches the peak point 2.89 GPa at $\varepsilon=0.0420$, then the model containing 2 prefabricated voids

Table 3 Specific parameters of models with different numbers of prefabricated voids
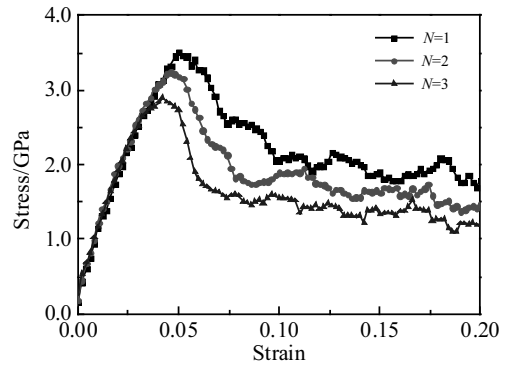
Number of voids, N	1	2	3
Void coordinates	$(5a_0, 5a_0, 5b_0)$	$(5a_0, 3a_0, 5b_0)$, $(5a_0, 7a_0, 5b_0)$	$(5a_0, 2a_0, 5b_0)$, $(5a_0, 5a_0, 5b_0)$, $(5a_0, 8a_0, 5b_0)$
Void spacing	-	$2a_0$	$1a_0$
Number of atoms to be deleted	61	128	182
Number of atoms left	11 939	11 872	11 818

Fig.8   Stress-strain curves under different numbers of voids (N)

Table 4 Specific parameters of models with different void distributions

Distribution	A	B	C
Number of voids, N	3	3	3
Void coordinate	$(5a_0, 2a_0, 5b_0)$, $(5a_0, 5a_0, 5b_0)$, $(5a_0, 8a_0, 5b_0)$	$(2a_0, 5a_0, 5b_0)$, $(5a_0, 5a_0, 5b_0)$, $(8a_0, 5a_0, 5b_0)$	$(2.5a_0, 2.5a_0, 5b_0)$, $(5a_0, 5a_0, 5b_0)$, $(7.5a_0, 7.5a_0, 5b_0)$
Void spacing	$3a_0$	$3a_0$	$3.54a_0$
Void direction	[010]	[100]	[110]
Angle to tensile direction	90°	0°	45°
Number of atoms to be deleted	182	182	182
Number of atoms left	11 818	11 818	11 818

In order to study the influence of the void distribution on the tensile mechanical properties of Al_2Cu, the tensile behavior along the X-axis of the model with three prefabricated voids arranged in different directions is simulated under the 300 K constant temperature condition. According to the data in Table 4, the initial models obtained after relaxation are preset with three different void distributions, which are classified into A, B, C. In the configuration of A, three prefabricated voids are uniformly distributed in the direction perpendicular to the stretching direction [010]. In the configuration of B, three prefabricated voids are uniformly distributed along the direction of the tensile direction, namely [100]. While in the configuration of C, three prefabricated voids are uniformly distributed in the direction of [110], with an angle of 45º to the tensile direction. The whole system deforms once every run time step. The engineering strain is 0.001 ps^{-1}, and the whole program runs 20 000 steps. During this period, the coordinates of the atoms, strain rate, temperature, kinetic energy, potential energy and stress are recorded every 200 steps. The atomic trajectories of A, B and C configurations are shown in Fig.9a, 9b, and 9c, respectively.

The stress and strain data obtained by operation is plotted as the stress-strain curves shown in Fig.10. As can be clearly

Fig.7   Initial models with different numbers of voids: (a) 1, (b) 2 and (c) 3

reaches its peak point 3.24 GPa at ε=0.0460, and the model containing only one prefabricated void finally reaches the peak point 3.52 GPa at ε=0.0498. It clearly shows that both the plasticity and tensile strength of Al_2Cu decrease to different degrees as the number of voids increases.

As can be seen from Fig.8, the three curves are relatively smooth and abrupt fluctuations do not appear. While compared with the influence of void size on Al_2Cu, the stress-strain curves show obvious fluctuation when the prefabricated void radius is R=$1a_0$, and the fluctuation is more remarkable with the increase of strain rate.

3.4   Influence of the prefabricated void distribution on Al_2Cu tensile results

seen, the starting points of the three curves are the same, which means that they have the same pre-stress of 0.26 GPa. This is because pre-stress is introduced by the free surface. Since the three models contain three prefabricated voids with the identical radius of $R=1a_0$, they should have the same free surface area and the pre-stress. It can also be observed that when the angle is 90°, Al$_2$Cu reaches the peak point 2.89 GPa at $\varepsilon=0.0420$. This peak point is 3.21 GPa at $\varepsilon=0.0440$ when the angle is 45°, and it is 3.54 GPa at $\varepsilon=0.0480$ when angle is 0°. It indicates that the smaller the angle between the line of voids
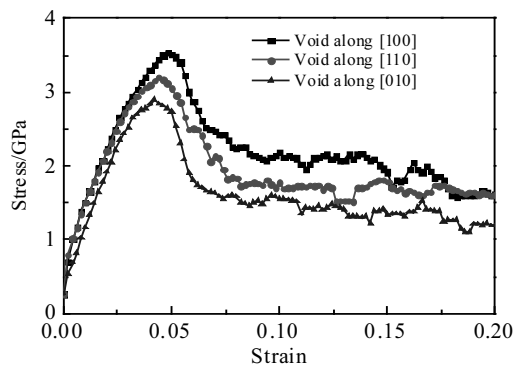
and the tensile direction, the stronger the plasticity and tensile strength of the Al$_2$Cu. There is no obvious difference in the stress-strain curves between the models with void spacing of $3a_0$ and $3.54a_0$.

4 Conclusions

1) Voids can create free surface in the model and the stress concentration is generated in the inner edge of the void, thus greatly reducing the tensile strength and deformation ability of the material. Plasticity and tensile strength of Al$_2$Cu decrease significantly with the increase of the void size, and the plastic flow occurs as the void increases to a certain extent.

2) Stress-strain curves corresponding to different numbers of voids are basically coincident in the elastic deformation stage, and the plasticity and tensile strength of Al$_2$Cu decrease to different degrees with the increase of void quantity.

3) The smaller the angle between the line of voids and the tensile direction, the stronger the plasticity and tensile strength of the Al$_2$Cu.

References

1   Zeng Yu, Yin Zhimin, Pan Qinglin *et al*. *Journal of Central South University, Science and Technology*[J], 2002, 33(6): 592 (in Chinese)

2   Zielinski A S, Chrzanowski J, Warmuzek M *et al*. *Materials and Corrosion*[J], 2004, 55(2): 77

3   Lukasak D A, Hart R M. *Light Metal Age*[J], 1991, 49(9): 11

4   Zhao Zhongkui, Zhou Tietao, Liu Peiying *et al*. *Materials Review*[J], 2006(7): 69

5   Gao Hongji, Xu Bin, Niu Yuchao *et al*. *Foundry Technology*[J], 2005(8): 703

6   Gao Ka, Li Shuangming, Fu Hengzhi. *Acta Metallurgica Sinica*[J], 2014, 50(8): 962

7   Tian Jinzhong, Zhao Yuhong, Hou Hua *et al*. *Solid State Communications*[J], 2017, 268: 44

8   Lombardi A, Mu W, Ravindran C *et al*. *Journal of Alloys and Compounds*[J], 2018, 747: 131

9   Sadeghi I, Wells A M, Esmaeili S. *Journal of Materials Processing Technology*[J], 2018, 251: 232

10 Zhang Junshan. *Strength of Materials*[M]. Harbin: Harbin Institute of Technology Press, 2004: 107

11 Dumont D, Deschamps A, Bréchet Y. *Materials Science and Engineering A*[J], 2003, 356(1-2): 326

12 Doyama M. *Nuclear Instruments and Methods Physics Research Section B*[J], 1995, 102(1-4): 107

13 Mäki-Jaskari M , Kaski K, Kuronen A. *Computational Materials Science*[J], 2000, 17(2-4): 336

14 Celik F A，Ozgen S, Yıldız A. *Molecular Simulation*[J], 2006, 36(6), 443

15 Cao Ajing, Wei Yueguang. *Physical Review B*[J], 2006, 74(21): 214 108

16 Zhang Xiaoyong, Zhang Bin, Li Chao *et al*. *Rare Metal Materials and Engineering*[J], 2013, 42(10): 2057
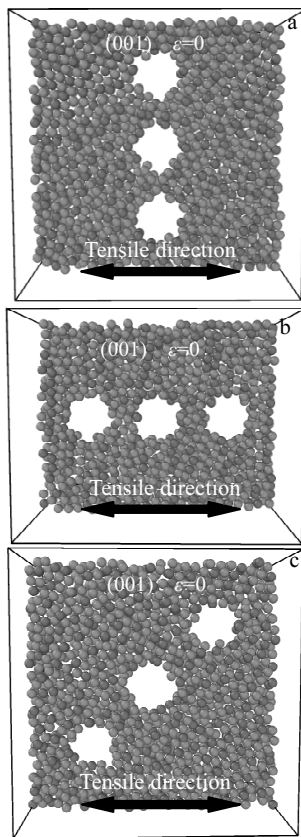
Fig.9   Models with different void distributions: (a) A, along [010]; (b) B, along [100]; (c) C, along [110]

Fig.10   Stress-strain curves of different void distributions

17 Yuan Lin, Jing Peng, Liu Yanhua *et al*. *Journal of Physics*[J], 2014, 63(1): 276

18 Liang Li, Ma Mingwang, Tan Xiaohua *et al*. *Acta Metallurgica Sinica*[J], 2015, 51(1): 107

19 Chen Jun, Xu Yun, Chen Dongquan *et al*. *Acta Physica Sinica*[J], 2008, 57(10): 6437

20 Bringa E M, Traiviratana S, Meyers M A. *Acta Materialia*[J], 2010, 58(13): 4458

21 Desai T G, Millett P, Tonks M *et al*. *Acta Materialia*[J], 2010, 58(1): 330

22 Zeng Xiangguo, Xu Shusheng, Chen Huayan. *Transactions of Nonferrous Metals Society of China*[J], 2010, 20(S2): 519

23 Zhang Ning, Yang Xinhua, Chen Chuanyao. *Chinese Journal of Computational Mechanic*[J], 2010, 27(2): 330

24 Simar A, Voigt H J L, Wirth B D. *Computational Materials Science*[J], 2011, 50(5): 1811

25 Liu Qunfeng, Shen Shengping. *Computational Materials Science*[J], 2013, 67: 123

26 Meetsma A, De Boer J L, Van Smaalen S. *Journal of Solid State Chemistry*[J], 1989, 83(2): 370

27 Daw M, Baskes M I. *Physical Review Letters*[J], 1983, 50(17): 1285

28 Wang Weidong, Yi Chenglong, Fan Kangqi. *Transactions of Nonferrous Metals Society of China*[J], 2013, 23(11): 3353

含孔洞的 Al$_2$Cu 单轴拉伸的分子动力学模拟

刘晓波，熊 震，方 洲，李 艳

(南昌航空大学，江西 南昌 330063)

摘 要：建立了含孔洞的 Al$_2$Cu 分子动力学模拟模型，采用嵌入原子法模拟 Al$_2$Cu 模型在常温、恒定工程应变速率的拉伸环境下孔洞大小、数量及孔洞分布对 Al$_2$Cu 力学性能的影响。结果表明：孔洞的出现使模型内部出现了自由表面并在孔洞内边缘产生了应力集中，从而大大降低材料的抗拉强度以及变形能力；孔洞增大，Al$_2$Cu 的塑性和抗拉强度均明显下降；不同孔洞数量对应的应力-应变曲线在弹性变形阶段基本重合，孔洞增多，Al$_2$Cu 的塑性以及抗拉强度都有不同程度的下降；改变孔洞分布，孔洞连线方向与拉伸方向的夹角越小，Al$_2$Cu 表现出越强的塑性和抗拉强度。

关键词：分子动力学模拟；拉伸；孔洞大小；孔洞数量；孔洞分布

作者简介：刘晓波，男，1963 年生，博士，教授，南昌航空大学航空制造工程学院，江西 南昌 330063，电话：0791-83953108，E-mail: liuxb2000@sina.com